Palaeogeography, Palaeoclimatology, Palaeoecology 441 (2016) 430–437

Contents lists available at ScienceDirect

Palaeogeography, Palaeoclimatology, Palaeoecology

journal homepage: www.elsevier.com/locate/palaeo

Link between cyclic eustatic sea-level change and continental weathering: Evidence for aquifer-eustasy in the Cretaceous

Jens E. Wendler [a,*], Ines Wendler [a], Christoph Vogt [b], Jochen Kuss [a]

[a] Department of Geosciences, Bremen University, P.O. Box 330440, 28334 Bremen, Germany

[b] Crystallography/Central Laboratory for Applied Material Sciences (ZEKAM), Department of Geosciences, Bremen University, P.O. Box 330440, 28334 Bremen, Germany

ARTICLE INFO

Article history:
Received 20 April 2015
Received in revised form 3 August 2015
Accepted 12 August 2015
Available online 20 August 2015

Keywords:
Hydrological cycle
Sequence stratigraphy
Terrigenous minerals
Greenhouse climate
Cenomanian
Turonian

ABSTRACT

Cyclic fluctuations in global sea level during epochs of warm greenhouse climate have remained enigmatic, because absence or subordinate presence of polar ice during these periods precludes an explanation by glacio-eustatic forcing. An alternative concept suggests that the water-bearing potential of groundwater aquifers is equal to that of ice caps and that changes in the dynamic balance of aquifer charge versus discharge, as a function of the temperature-related intensity of the hydrological cycle, may have driven eustasy during warm climates. However, this idea has long been neglected for two reasons: 1) the large storage potential of subsurface aquifers was confused with the much smaller capacity of rivers and lakes and 2) empirical data were missing that document past variations in the hydrological cycle in relation to eustasy.

In the present study we present the first empirical evidence for changes in precipitation, continental weathering intensity and evaporation that correlate with astronomically (long obliquity) forced sea-level cycles during the warmest period of the Cretaceous (Cenomanian–Turonian). We compare sequence-stratigraphic data with changes in the terrigenous mineral assemblage in a low-latitude marine sedimentary sequence from the equatorial humid belt at the South-Tethyan margin (Levant carbonate platform, Jordan), thereby avoiding uncertainties from land–ocean correlations. Our data indicate covariance between cycles in weathering and sea level: predominantly chemical weathering under wet climate conditions is reflected by dominance of weathering products (clays) in deposits that represent sea-level fall (aquifer charge > discharge). Conversely, preservation of weathering-sensitive minerals (feldspars, epidote and pyroxenes) in transgressive sediments reflects decreased continental weathering due to dryer climate (aquifer discharge > charge). Based on our results we suggest that aquifer-eustasy represents a viable alternative to glacio-eustasy as a driver of cyclic 3rd-order sea-level fluctuations during the middle Cretaceous greenhouse climate, and it may have been a pervasive process throughout Earth history.

1. Introduction

Rhythmic fluctuation of global sea level on orbital time scales during the Cretaceous has been suggested repeatedly and demonstrated by spectral analyses (Laurin and Sageman, 2007; Wendler et al., 2010; Boulila et al., 2011; Wendler et al., 2014; Laurin et al., 2015). While, on timescales $>10^6$ years, solid Earth processes like plate tectonics influence sea level via changes in the ocean basin volume, on orbital timescales, sea level is dominated by changes in the volume of ocean water due to climate forcing (see review by Conrad 2013). The increasing evidence of a globally synchronous sea-level forcing on orbital timescales (10^4 to 10^6 years) raises the question: Which cyclic components of the hydrological cycle controlled the distribution of water between the oceans and the continents in the Cretaceous?

For icehouse climate epochs, sea-level fluctuations are explained by the repeated build-up and melting of polar ice caps. This mechanism has been proposed to control sea level also during the Cretaceous greenhouse climate, based on the assumption that it is a pervasive process in both icehouse and greenhouse (Miller et al., 2005a; Miller et al., 2005b) climate modes of the Earth (see also Wendler and Wendler, 2016). Invoking solely glacio-eustasy to explain sea-level change throughout Earth history is tempting for two reasons: 1) Storage of water in ice caps is understood and modelled relatively thoroughly due to the immense database from studies of the recent icehouse epoch. 2) The evidence of sustained warmth with ice-free poles during the Cretaceous greenhouse epoch (Huber et al., 2002; Moriya et al., 2007; Francis et al., 2008; MacLeod et al., 2013) is challenged by the possible presence of ice sheets, especially if these supposedly occurred during the warmest period of the Cretaceous, i.e. the Cenomanian and Turonian (Stoll and Schrag, 2000; Bornemann et al., 2008; Galeotti et al., 2009).

* Corresponding author. Tel.: +49 421 218 65132; fax: +49 421 218 65159.
E-mail address: wendler@uni-bremen.de (J.E. Wendler).

http://dx.doi.org/10.1016/j.palaeo.2015.08.014
0031-0182/

The controversy on glacio-eustatic sea-level control during the middle Cretaceous warm greenhouse climate raises the question whether build-up of ice sheets is the only process that can significantly change the volume of ocean water. Based on mass balance calculations, it was suggested that another important reservoir is storage of groundwater in aquifers, with a capacity that is at least as high (26.35×10^6 km^3; Trenberth et al., 2007) as the water volume currently bound in ice (Hay and Leslie, 1990). These estimates gave rise to the hypothesis that changes in the global groundwater reservoir could cause eustatic sea-level changes (Hay and Leslie, 1990; Jacobs and Sahagian, 1993, 1995; Wendler et al., 2011). The hypothesis of groundwater-forced sea-level fluctuations, termed aquifer-eustasy (Wendler and Wendler, 2016) or limno-eustasy (Wagreich et al., 2014), had been widely neglected due to underestimation of the capacity of subsurface aquifers (116×10^6 km^3; Hay and Leslie, 1990), probably by confusing it (Fig. 1 in Miller et al., 2005a) with the low water volume of $0.03–0.3 \times 10^6$ km^3 in lakes and rivers (Hay and Leslie, 1990). Because the Greek word "limne" translates as "lake", the term limno-eustasy may provoke an association with surface aquifers only, which would disregard subsurface aquifers that are the principle storage medium for groundwater-forced sea-level fluctuations. In order to avoid such etymological confusion we prefer to use the term aquifer-eustasy.

Feasibility of aquifer-eustatic forcing of cyclic 3rd-order sea-level changes in the Cretaceous can be tested with numerical model approaches and by identification of sedimentological evidences for varying transfer of water from the oceans to the continents. Modelling the rate of charge and discharge of aquifers for the Cretaceous has been difficult because of three main unknowns (Hay and Leslie, 1990): 1) the unknown potential of Cretaceous aquifers that mostly got eroded or buried, 2) uncertainty about possible climate fluctuations that could change evaporation/precipitation sufficiently on the required time-scales, and 3) effectiveness of infiltration and discharge of any given aquifer. In the present study, we follow the alternative approach of an empirical test, by using direct observations in the sedimentary record that indicate changes in precipitation and weathering. A causal link between sea level and precipitation is expected to generate a sea-level rise during precipitation decrease, and vice versa. Variability in precipitation can be assessed qualitatively from the mineral-assemblage signal of weathering intensity of the eroded rocks and soils that are transported as siliciclastic input into the marine sediments.

For such analyses, shallow-marine settings are well suited, because they are close to the source of terrestrial influx and most sensitive to sea-level fluctuations. However, in these sequences it has been difficult to proof the presence of astronomical cycles and their relation to sea level, because of unsteady sedimentation and absence of radio-isotopic constraints. Using Evolutive Average Spectral Misfit time series analysis, specifically designed to rigorously test for astronomical forcing under such conditions, a major advance was achieved in a recent study (Wendler et al., 2014) of a shallow-water carbonate section from the Levant Platform in Jordan. For that same sequence-stratigraphically and astrochronologically well-constrained section, we employ a full quantification of the mineral assemblage in order to test for synchronicity in precipitation-related weathering of minerals and sea-level fluctuations.

We explore such changes in hinterland weathering intensity over four 3rd-order sea-level cycles of a marine Cenomanian–Turonian carbonate platform section that spans ~5 Myr (Wendler et al., 2014). Importantly, this approach has the advantage of studying both terrestrial (siliciclastics) and marine (carbonates and evaporites) signals from mineral assemblages as climate proxies in one and the same section, thereby avoiding correlation uncertainties between marine and continental (e.g. lake levels) records. Furthermore, the investigated section is particularly suitable for our approach for two reasons: 1) It has a paleogeographic position (Fig. 1) that restricts possible source areas for terrigenous siliciclastics (weathered material) to the tropical humid belt; 2) It was positioned in the northern hot arid belt (Hay and Floegel, 2012) during the Cenomanian–Turonian, so that the marine sediments yield indicators for evaporation changes in relation to sea level. While the carbonates and evaporites represent the climate conditions and sea level on the platform, the siliciclastic components reflect the climate conditions in the hinterland. Determination of the complete siliciclastic assemblage enables us to record both the source minerals and the weathering products (clays). The relative contribution of these two mineral groups is used as an indicator for weathering intensity.

2. Material and methods

Section GM3 in Jordan (Ghawr Al Mazar or Ghor al Mazrar: 31°15′34′′ N; 35°35′41′′ E) represents a platform carbonate sequence that was deposited on the rimmed Levant Carbonate platform at approximately 100 km distance from the palaeo-coastline of the Arabian Shield (Fig. 1). The section contains open-marine subtidal to supratidal deposits and was sampled at a sample interval of 10 to 30 cm. More detailed information on the lithology and biostratigraphy is given in Wendler et al. (2014) and references therein. Stable carbon-isotope

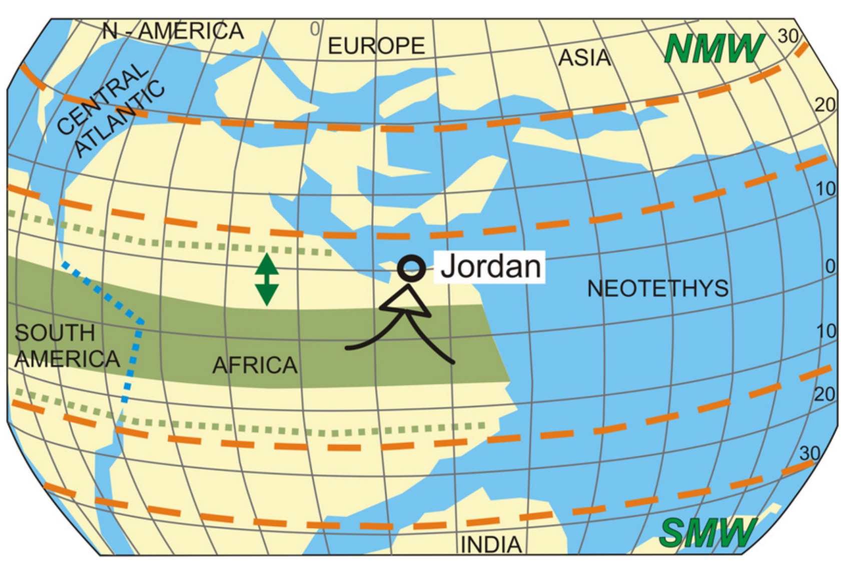

Fig. 1. Paleogeography of the studied GM3 section in Jordan (after Cavazza et al., 2004). Circle: section position; arrow indicates origin of siliciclastic input. Approximate Turonian–Santonian climate belts (Chumakov, 1995; Hasegawa et al., 2012; Hay and Floegel, 2012); green: equatorial humid belt with maximal expand (green dotted lines, green arrow); orange dashed lines: northern and southern hot arid belts; NMW = Northern Mid-latitude Warm humid belt, SMW = Southern Mid-latitude Warm humid belt.

ratios (378 samples) were measured on bulk carbonate using a Finnigan MAT 251 mass spectrometer. The results are reported relative to the Vienna Pee Dee belemnite standard (V-PDB) at analytical precision better than ±0.05‰.

Mineral assemblages, for 125 samples at a sample interval of 1 m, were determined using X-ray diffraction pattern analyses at the laboratories of the research group Crystallography (University of Bremen, Central Laboratory for Crystallography and Applied Material Sciences, ZEKAM, Dept. of Geosciences). Dried bulk samples were powdered (<20 μm particle size) and prepared with the Philips back-loading system. For mineral groups that constitute >20% of the clay fraction a standard deviation of ±5% can be considered a conservative guideline for bulk sample powder analysis (Moore and Reynolds, 1997). The determination of well crystallized minerals like quartz, calcite or aragonite has a standard deviation better than ±5% (Tucker, 1988; Vogt et al., 2002). X-ray diffractograms were measured on a Philips X'Pert Pro multipurpose diffractometer equipped with a Cu-tube (k_α 1.541, 45 kV, 40 mA), a fixed divergence slit of ¼°, a 16 samples changer, a secondary Ni filter and the X'Celerator detector system. The measurements were done as a continuous scan from 3 to 85° 2θ, with a calculated step size of 0.016° 2θ (calculated time per step was 100 s). Mineral identification was performed using the Philips software X'Pert HighScore™ and identification of sheet silicates was done with the Apple MacIntosh X-ray diffraction interpretation freeware MacDiff 4.25 (http://www.geologie.uni-frankfurt.de/Staff/Homepages/Petschick/Rainer.html#MacDiff; Petschick et al., 1996). This was followed by a full quantification of the mineral assemblage of the bulk fraction via the QUAX full pattern method (c.f. Vogt et al. 2002).

Determination of clay minerals is based on more than 100 reference mineral patterns for clay minerals in the current QUAX database version. Reference clay minerals are related to mineral groups, depending on their original description and naming, which might be different when following traditional grouping according to the common routine for the analysis of clay mineral composition: 1) separation of the clay fraction, 2) treatment of the clay fraction to get rid of carbonates, opal, amorphous Fe–Mn-Hydroxides, and 3) semi-quantitative estimation of the four clay mineral groups (smectites, illites, kaolinite, chlorites) according to e.g. (Biscaye, 1964, 1965). It should be noted that, for the present study, the clay mineral content was determined for the bulk fraction. Results for nearly amorphous material are based on various opaline reference patterns.

Raw XRD data were normalized to extract the three mineral groups focussed on in this study (wt% of the individual minerals within each grouping summed to 100%): siliciclastic minerals, clay minerals and carbonate/sulphate minerals (Fig. 2, panels b–d). Thereby, the influence of major fluctuations in carbonate content is reduced. The raw data are available at Pangaea geological data base www.pangaea.de.

3. Results and discussion of the mineral assemblage

3.1. Indicators for weathering and evaporation

The data presentation of this study (Fig. 2, panels b–d) focuses on changes in the amount of weathering-sensitive minerals (WSM) of the siliciclastic assemblage, used as an indicator for weathering intensity (Fig. 2b). The WSM comprise feldspars and heavy minerals, the latter represented by epidote, pyroxenes and amphibols. These minerals are directly derived from the source rock and must be deposited rapidly in order to be preserved, thus lag times are minimal as opposed to the weathering products, i.e. the clay minerals (Fig. 2c). The latter are formed during weathering and soil formation, so that lag times between their formation and final deposition in a marine sequence can be up to a million years (Thiry, 2000). After taking into account this time lag and upon careful evaluation of diagenetic influences, the clay mineral assemblage can give valuable climate information (Singer, 1984; Chamley, 2001) from the hinterland. The third mineral group that is considered comprises the carbonates and sulphates (Fig. 2d). These minerals represent the local marine signals of the evaporitic component of the hydrological cycle.

3.2. Relation between distribution patterns of siliciclastic minerals, weathering and sea level

A cyclic fluctuation in the relative abundance of WSM, clay minerals and carbonates/sulphates in relation to the 3rd-order depositional sequences is evident from Fig. 2. The WSM change significantly in relative abundance, whereas quartz (largely insensitive to chemical weathering) occurs at a relatively constant percentage in the siliciclastic assemblage throughout the section (Fig. 2b). The proportion of weathering products versus WSM increases upon strong chemical weathering (Bergaya et al., 2006). The highest percentages of weathering products occur during the sea-level highstands and lowstands, i.e. during the regressive intervals, which suggests that enhanced precipitation fuelled chemical weathering during these times. The transgressions, on the contrary, are characterized by higher percentages and partially a dominance of WSM, suggesting decreased weathering and, hence, dryer conditions in the continental source area in conjunction with sea-level rise.

To evaluate these results critically, two aspects require further consideration: 1) the proportion of clays in general is high throughout the section, pointing at persistent strong chemical weathering, as would be expected for the near-equatorial source area under greenhouse conditions. The transgressions, in fact, appear as relatively rapid, pulse-like (Wendler et al., 2014) "dry" episodes in this overall humid climate pattern. 2) It could be argued that the roughly positive correlation between increased percentages of WSM and limestone beds (for wt% carbonate see Wendler et al., 2014) is caused by a methodological error that gives different XRD results for WSM at variable carbonate contents. We can exclude this possibility, because decalcified duplicates of limestone samples yield comparable results. In addition, this correlation is not consistent and disappears in the limestone sequences at 20–25 m and 110–120 m. This observation, and the constancy in quartz, contradict also the possibility that relative fluctuations within the siliciclastic assemblage could solely be reflections of the total clay content.

An alternative interpretation would be a predominant diagenetic influence on the siliciclastic assemblage. However, a diagenetic process that resulted in preservation of chemically sensitive minerals over clay minerals in the limestone seems counter-intuitive, because a stronger diagenetic alteration by pore waters is expected to occur in the more porous limestone beds as compared to the marls. Furthermore, it is widely accepted that very little shallow-burial early-diagenetic influence affects the clay mineral assemblage after its storage in sediments (Chamley, 2001). Concluding, the proportion of WSM in the siliciclastic fraction is indeed higher in the limestone intervals and points to synchronism between marine carbonate formation and reduced chemical weathering in the hinterland.

Kaolinite represents the prime product of chemical weathering (Biscaye, 1964; Singer, 1984; Thiry, 2000; Chamley, 2001) and forms preferably under warm and humid climates (Hallam et al., 1991), i.e. enhanced hydrological cycling. In contrast, the weathering products illite and mica represent physical weathering (Chamley, 2001) and coincide with peaks of WSM, predominantly in the transgressive intervals (Fig. 2b and c). Therefore, the transgressive phases with their increased percentage of illite and WSM can be interpreted to represent a shift in the dominance from chemical to physical weathering. This shift led to the presence of non-chemically weathered siliciclastica in the river loads, without a significant time lag. Thus, as would be expected from the theory of aquifer-eustasy (Fig. 3), we observe an alternation in the clay mineral assemblage in conjunction with sea-level fluctuations that likely reflects changes in precipitation and weathering.

Besides climatic factors, the clay mineral assemblage is influenced also by coast line proximity and differential settling related to grain size, grain shape and freshwater versus saline water density gradients

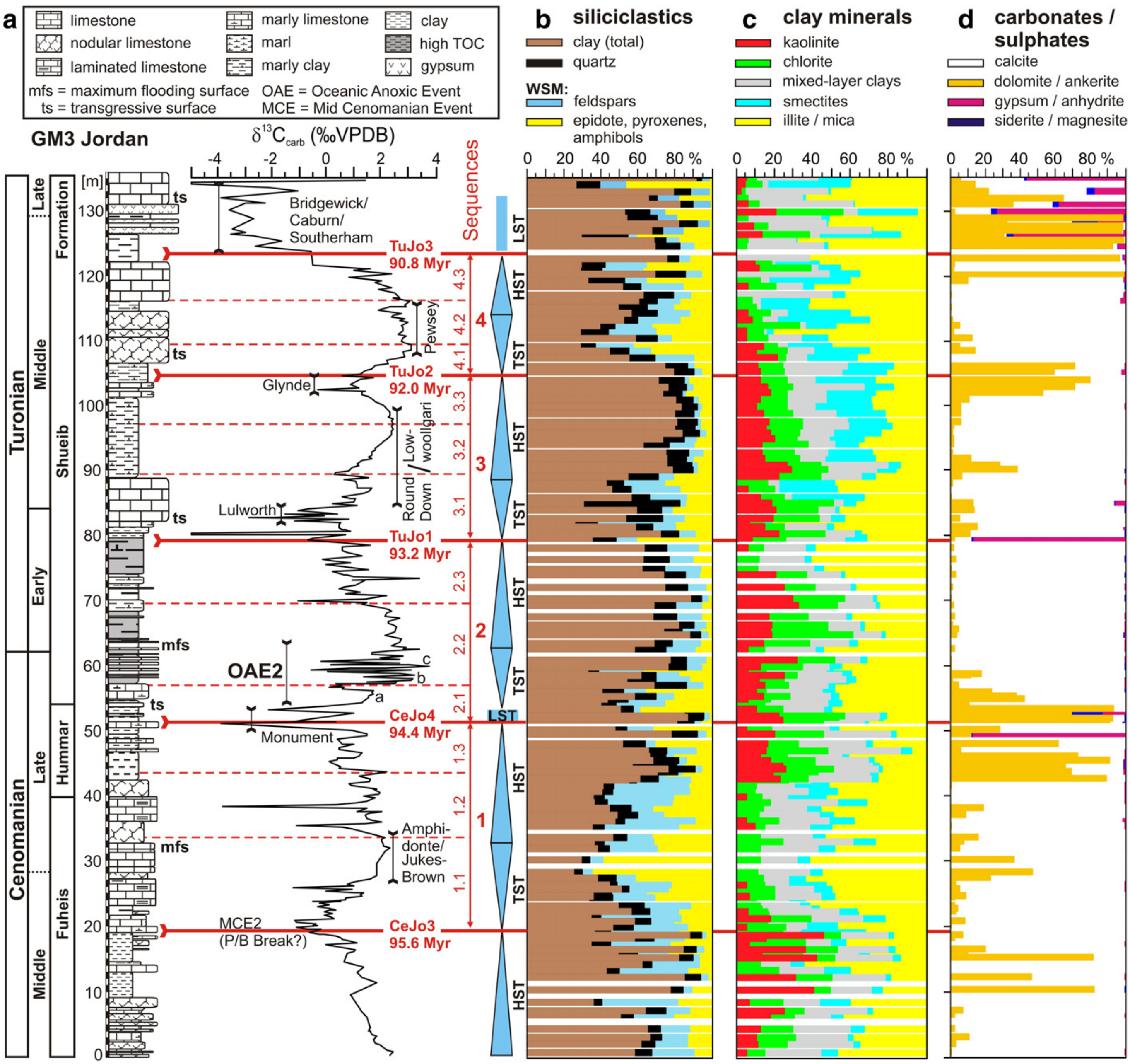

Fig. 2. Data from mineral assemblage analyses in relation to sequence stratigraphy for the GM3 section in Jordan. a) Stratigraphic profile and $\delta^{13}C$ stratigraphy (main isotope-events with ranges; for biostratigraphy see Wendler et al., 2014). Sequence stratigraphy and sea-level cycles (Wendler et al., 2014): 3rd order (solid red lines) and 4th-order (dashed red lines) sequence boundaries, e.g. CeJo4 = fourth Cenomanian sequence boundary of Jordan. Four numbered 3rd-order sequences with ages (1.2 Ma obliquity cycles) provide floating astrochronological timescale (Wendler et al., 2014), tied to the radiometric Cenomanian–Turonian boundary age of 93.9 Myr; TST = Transgressive Systems Tract, HST = Highstand Systems Tract, LST = Lowstand Systems Tract. b) Siliciclastic mineral assemblage (normalized to total siliciclastics). Note increased rates of WSM in correspondence to sea-level highs (TST). c) Clay mineral assemblage (normalized to total clay minerals). Note that peaks in illite/mica correspond to peaks of WSM in panel b and to sea-level rise; minima in illite/mica are associated with sequence boundaries. d) Carbonate and sulphate mineral assemblage. Note broad dolomite intervals and gypsum beds associated with sequence boundaries.

(Singer, 1984). Preferential settling of the finer material during sea-level highstand (more distal setting) has been attributed to higher abundance of illite, because it is often observed to be finer-crystalline relative to kaolinite (Singer, 1984). However, this interpretation is excluded by the combined occurrence of high amounts of illite together with an increase in heavy minerals during the transgressive intervals, because the latter would preferentially settle in more proximal settings. Instead, the presence of abundant illite along with WSM supports the scenario of dryer conditions during the transgressive phases (Fig. 3b).

Interestingly, the variability in the siliciclastic minerals shows also a tendency to follow the fourth order sequences (405 kyr eccentricity cycle, Wendler et al., 2014; dashed lines in Fig. 2). This points at higher-frequency wet/dry climate variability that may be associated also with variations in runoff paths (areal precipitation changes), similar to known precession-scale monsoonal cycles (Pachur and Kroplein, 1987; Jacobs and Sahagian, 1995) or shifts in meridional climate belts (Schmidt and Spero, 2011).

3.3. Relation between distribution patterns of authigenic marine minerals and sea level

The authigenic marine mineral assemblage at the sequence boundaries and in the lowstand deposits reveals significant amounts of gypsum at CeJo4, TuJo1 and TuJo3 (Fig. 2a and d), sometimes associated

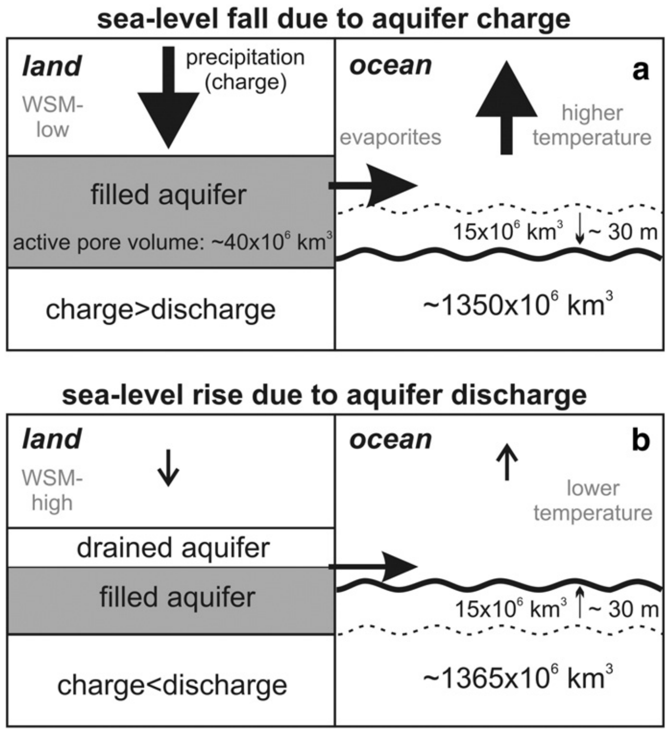

Fig. 3. Scheme of aquifer-eustasy. Illustrated are changes in dynamic groundwater volume and sea level as a function of the balance between evaporation, precipitation (strength and/or areal expand) and runoff (surface water and groundwater discharge). a) Eustatic regressions; b) eustatic transgressions. Note: Involved are the upper parts of aquifers that participate actively in the groundwater charge/discharge. Indicated is the estimated active pore volume for Cretaceous sediments that were 200 m above present day sea-level and assuming 1000 m average continental elevation (Hay and Leslie, 1990). The ocean water volume for a hypothesized ice-free world is given as the sum of modern ocean water volume and ice volume, according to estimates by Trenberth et al. (2007).

with massive gypsum with chickenwire texture and tepee structures. This signature suggests strong evaporation and enhanced landward transport of water (continental precipitation) in conjunction with falling sea level, as would be expected from the hypothesis of aquifer-eustasy (Fig. 3a). Of course, such a pattern could be caused also by local facies shifts and related increased evaporation due to establishment of restricted conditions that may occur as a result of lowered sea level. However, the platform-wide occurrence of sabkha deposits, particularly at TuJo3 (Schulze et al., 2004; Wendler et al., 2014), argues against a locally restricted facies shift to have caused the formation of evaporites at the studied location.

The second marine mineral group are the carbonates. In the studied section, these are mainly composed of calcite, whereas dolomites are present in several-metre thick intervals that include four of the five 3rd-order sequence boundaries and deposits of the associated late highstands and lowstands (Fig. 2d). The sabkha brines, from which the gypsum precipitated, were potential media also for reflux processes that formed the dolomites, considering the combination of enhanced fluvial runoff and high evaporation during an intensified hydrological cycle (Fig. 3a). That the dolomites in the Jordan section were influenced by this combined meteoric water–brine dolomitization type is supported by their stable-isotopic signature of very high $\delta^{18}O$ and low $\delta^{13}C$ values (Wendler et al., 2014), which is typical for such dolomites (Allen and Matthews, 1982) and comparable with the isotopic signature from Permian (Magaritz and Peryt, 1994; Peryt and Scholle, 1996) and recent (Pierre et al., 1984) dolomites that were formed in environments with mixing of highly saline and freshwater. For the studied section, such a scenario is further supported by palaeoecological evidence that indicates rapid alternation between hypersaline and brackish conditions at sequence boundary CeJo4 (Morsi and Wendler, 2010). Such varying dominance in runoff and strong evaporation during late highstands and lowstands (Morsi and Wendler, 2010; Wendler et al., 2014) is in line with the hypothesis that intensification of the hydrological cycle under warmer temperatures caused a landward shift in the ocean–continent water balance and forced sea-level regressions (Fig. 3a).

4. The concept of aquifer-eustasy

4.1. Dynamic balance of aquifer charge versus discharge

In the sections above, we demonstrate that the mineral assemblage of a Cenomanian–Turonian record from a low-latitude carbonate platform reveals variations in continental weathering intensity that suggest precipitation changes in synchrony with cyclic, astronomically-driven 3rd-order sea-level changes. These observations provide compelling evidence for aquifer-eustatic forcing of sea-level changes during the middle Cretaceous warm greenhouse climate.

Aquifer-eustasy operates through precipitation-forced dynamic balance in the distribution of water between ocean and land that is driven by cyclic, temperature-related variations in the strength of the hydrological cycle (Fig. 3). A relative decrease in precipitation causes dominance of aquifer discharge (fluvial runoff) over aquifer charge (precipitation) and thus an oceanward shift in this balance, resulting in transgression (Fig. 3b). The associated dryer conditions are reflected by enhanced preservation of WSM due to decreased continental weathering in the continental source areas of siliciclastic sediments (Fig. 2b). Conversely, regressions are caused by a landward shift in the ocean–land water balance through an intensified hydrological cycle under warmer temperatures, and are associated with increased precipitation and enhanced chemical weathering (Fig. 3a). Because increased precipitation requires enhanced marine evaporation, enhanced formation of dolomites and sulphates occurs during sea-level fall (Fig. 2d).

Emphasis must be put on the more dynamic nature of storage of liquid water in continental surface and subsurface reservoirs, as opposed to the more static storage of water in its solid state within continental ice sheets. This means that the concept of aquifer-eustasy does not require any long-term water storage in a static sense. Instead, it considers the net storage that results from the dynamic balance between aquifer charge due to precipitation and discharge due to fluvial runoff. Any imbalance between these two processes causes a shift in the distribution of water between continents and oceans, and thus a change in global sea level (Fig. 3). This dynamic balance further implies that aquifer-eustatic regressions require a sustained dominance of aquifer charge over discharge, through increased areal expand and/or amount of precipitation (see Section 4.4). Modelling the speed and volume of aquifer charge/discharge is hampered by uncertainties in size estimates of the global water reservoirs. While beyond the scope of the present study, numerical simulation of aquifer-eustasy should be attempted in future research.

4.2. The potential of aquifer-eustasy

As an important prerequisite for correct mass balance evaluation, the storage estimates for the Cretaceous need to exclude those aquifers below 200 m continental elevation that were unavailable for charge/discharge, because of epicontinental flooding by an up to 200 m higher Cretaceous sea level (Conrad, 2013). Conservative estimates (Hay and Leslie, 1990) take into account the available volume, pore space parameters, and retention times of aquifers above 200 m average elevation of the groundwater table. These estimates indicate a water bearing capacity of ~20×10^6 km^3, when applying the modern average pore volume and available land surface area, capable of lowering global sea level by ~40 m, including isostatic adjustment. For comparison, a volume of 15×10^6 km^3 of water would be required to cause ~30 m of sea-level change, i.e. the average amplitude of 3rd-order sea-level fluctuations during the middle Cretaceous (Cenomanian, Turonian; Miller et al., 2005a; Voigt et al., 2006).

Cretaceous aquifers above sea level probably consisted to a higher percentage of younger, more porous sediments, so that their potential pore volume could have been twice that of today's aquifers (~40×10^6 km^3; Hay and Leslie, 1990). In addition, the expand of deserts during greenhouse conditions was probably smaller than today, and ice-free polar regions were available for aquifer charge, in contrast to modern high-latitude areas that are locked by permafrost and ice coverage. It can further be assumed that an enhanced hydrological cycle due to higher global temperatures during the Cretaceous transported more water towards these high latitudes, providing the water to fill the available pore space. These arguments suggest that Cretaceous aquifers had the potential to have caused also the larger Cretaceous 3rd-order sea-level changes of ~70–100 m that were proposed, e.g., for the latest Middle Turonian (Haq, 2014). In summary, the volume of available pore space in sedimentary rocks on land combined with an intense hydrological cycle provides a tremendous potential for continental water storage in the absence of polar ice caps during the middle Cetaceous warm greenhouse climate.

4.3. Aquifer-eustasy during Oceanic Anoxic Event 2 (OAE2)

Because the OAE2 was an overall humid period with accelerated hydrological cycling (e.g.van Helmond et al., 2014), the aquifer-eustatic prediction of humidity-driven landward water transfer (regression) seemingly contradicts the long-term sea-level rise that is indicated for this period. However, OAE2 is a special case because it is considered to represent a period of hothouse climate, during which whole ocean thermal expansion can drive a few tens of metres of sea-level rise (Kidder and Worsley, 2010). These steric effects may have forced the long-term transgression during OAE2, while the aquifer-eustatic process probably continued in the background independently (see also Wendler and Wendler, 2016). This assumption is supported by evidence of increased aridity in relation to eustatic sea-level rise on higher-frequent cyclicity during OAE2 (Mort et al., 2007; Gertsch et al., 2010; Wendler et al., 2011).

Also the present study shows that, in detail, a three-fold transgression/regression sequence is observed during OAE2 (4th-order sequences 2.1, 2.2. and 2.3 in Fig. 2; Wendler et al., 2014), consistent with results from German sections (Richardt et al., 2013). These fluctuations indeed continue to be related to changes between humid and dryer phases. Sequence 2.1 represents the initial transgression of OAE2 and is associated with carbon isotope peak "a" (Fig. 2). For this sea-level rise, dryer conditions and decreased terrigenous influx were widely shown (Mort et al., 2007; Elrick et al., 2009; van Helmond et al., 2014), representing the pattern that would be expected from aquifer-eustatic forcing. Thus, the sea-level record of OAE2 represents a combined signal of thermal expansion of ocean water, caused by volcanism-induced warming, and aquifer-eustatic forcing that most likely is astronomically controlled, as discussed below.

4.4. Driver of aquifer-eustasy

A possible driver of aquifer-eustasy involves changes in areal distribution and amount of precipitation due to spatiotemporal shifts in the latitudinal expand of arid and humid zones (Fig. 1) that are controlled by the Hadley circulation. Recent studies suggest that CO_2/temperature-driven shrinkage/expansion (sudden jump of 15° latitude) of the Hadley circulation, with possible consequences for the width of the intertropical convergence zone (ITCZ, equatorial humid belt), have controlled long-term spatial moisture distribution during the Cretaceous greenhouse climate (Hasegawa et al., 2012; Hay and Floegel, 2012). If this process acted at the time scale of 3rd-order sea-level fluctuations, such spatiotemporal shrinking of the humid zones would have diminished the areal expand of aquifer charge and, hence, would have caused a shift in net water balance towards rising sea level. There is indication for Holocene changes in the position and/or the width of the ITCZ on precessional scale (Collins et al., 2011; Schmidt and Spero, 2011). In this respect, cyclic variations in areal expansion and strength of monsoonal precipitation can be considered a key factor for aquifer-eustasy (Jacobs and Sahagian, 1993, 1995). It should be stressed that estimates of the land–ocean water balance need to consider not only the modulation of precipitation intensity, but also, and perhaps more importantly, the geographical distribution of precipitation.

4.5. Further evidences for aquifer-eustatic forcing of Cretaceous sea-level changes

While the potential of aquifer-eustatic forcing mainly relies on storage of groundwater in subsurface aquifers, further continental water reservoirs must have recorded the changes in precipitation. The process of aquifer-eustasy predicts that continental lake-level lowstands correlate with marine sea-level transgressions. Such correlation has indeed been reported from the continental Songliao Basin (China). Using the astrochronology and sequence stratigraphy (Wendler et al., 2014) of the section presented here, it was shown that Turonian–Santonian continental lake-level changes do not covary with marine sea-level changes (Wagreich et al., 2014). Instead, the lake-level highstands are associated with black shale events and correlate with major marine sequence boundaries that are recognized on global scale, which indicates that the amount of water on land correlates negatively to the amount of water in the oceans, as predicted from aquifer-eustasy.

The results from the Songliao Basin represent a paleo-latitude of ~65° N and suggest validity of the aquifer-eustatic process at high latitudes (mid- and high-latitude temperate humid belts). In analogy, but within a different context, an influence of humid/arid climate changes on the net water balance between the oceans and the continents has been proposed also for the Early Cretaceous (Föllmi, 2012). Furthermore, Wendler et al. (2016) present a sequence-stratigraphic analysis and foraminiferal $\delta^{18}O$ data for Turonian marine sediments from Tanzania that lends support to aquifer-eustatic forcing of sea-level changes during the middle Cretaceous, by showing that warmer temperatures occurred during the lowstands, whereas cooler temperatures prevailed during the transgressive intervals. Their study integrates sedimentological, paleontological and stable-isotopic evidence for an enhanced hydrological cycle during warmer periods to have caused both enhanced fluvial runoff (higher supply of freshwater, clastic sediments and nutrients) and a net transfer of water from the oceans to terrestrial aquifers that lead to eustatic sea-level fall. Similar integrated studies are needed to further test/consolidate the concept of aquifer-eustatic forcing of global sea-level changes under greenhouse climate conditions in the absence or subordinate importance of continental ice sheets (for a discussion of aquifer-eustasy in relation to climate modes see Wendler and Wendler, 2016).

5. Conclusions

The mineral assemblage of a Cenomanian–Turonian record from a low-latitude carbonate platform reveals cyclic alternations that are coeval with astronomically driven sea-level changes. These results represent the first robust empirical evidence for aquifer-eustatic forcing of sea-level changes in the middle Cretaceous. The process of aquifer-eustasy is based on a dynamic balance between charge (precipitation) and discharge (fluvial runoff) of surface and subsurface aquifers, reflecting the intensity of the hydrological cycle.

Preservation of WSM in the deposits of transgressive intervals indicates decreased continental weathering under dryer climate conditions and emptying of aquifers that caused eustatic sea level to rise. Inversely, the late highstand and lowstand deposits are characterized by dominance of clay in the siliciclastic fraction and elevated percentage of kaolinite, reflecting increased chemical weathering under more humid conditions in the hinterland. These observations, together with the occurrence of marine dolomites and evaporates, suggest an enhanced hydrological cycle and charging of aquifers that caused eustatic sea level to fall.

The cyclic shifts in water distribution between oceans and continental aquifers have sufficient capacity to potentially have caused the magnitudes of 3rd-order sea-level changes that are estimated for the middle Cretaceous. These shifts are thought to be driven by variations in areal expansion and strength of precipitation that are astronomically controlled. The present study indicates that aquifer-eustatic forcing of the mid-Cretaceous 3rd-order global sea-level changes was related to the long obliquity cycle, but this process probably controlled sea level also on shorter time-scales, as indicated form the literature.

The concept of aquifer-eustasy provides a plausible explanation for sea-level fluctuations during greenhouse climate modes when persistent, rhythmic glacio-eustatic fluctuations are unlikely. In fact, aquifer-eustasy might be a pervasive process throughout Earth history (Jacobs and Sahagian, 1995; Wendler and Wendler, 2016).

Acknowledgements

This research was funded by the German Science Foundation (DFG) grants KU 642/B20-1 and WE 4587/1-1. The QUAX development was supported by DFG grants Fi442/10-1,2,3,4 and Fi442/13-1,2 to C.V.s work. We thank A. Masri of the Jordan Geological Survey (NRA) for field assistance. This paper is a contribution to UNESCO-IUGS IGCP project 609 "Climate-environmental deteriorations during greenhouse phases: Causes and consequences of short-term Cretaceous sea-level changes".

References

Allen, J.R., Matthews, R.K., 1982. Isotope signatures associated with early meteoric diagenesis. Sedimentology 29, 797–817.
Bergaya, F., Theng, B.K.G., Lagaly, G., 2006. Handbook of Clay Science. Elsevier, Amsterdam.
Biscaye, P.E., 1964. Distinction between kaolinite and chlorite in recent sediments by X- ray diffract ion. Am. Mineral. 49, 1281–1289.
Biscaye, P.E., 1965. Mineralogy and sedimentation of recent deep-sea clays in the Atlantic Ocean and adjacent seas and oceans. Geol. Soc. Am. Bull. 76, 803–832.
Bornemann, A., Norris, R.D., Friedrich, O., Beckmann, B., Schouten, S., Sinninghe Damsté, J.S., Vogel, J., Hofmann, P., Wagner, T., 2008. Isotopic evidence for glaciation during the Cretaceous supergreenhouse. Science 319, 189–193.
Boulila, S., Galbrun, B., Miller, K.G., Pekar, S.F., Browning, J.V., Laskar, J., Wright, J.D., 2011. On the origin of Cenozoic and Mesozoic "third-order" eustatic sequences. Earth Sci. Rev. 109, 94–112.
Cavazza, W., Roure, F., Spakman, W., Stampfli, G.M., Ziegler, P.A., 2004. The TRANSMED Atlas.
Chamley, H., 2001. Clay Mineralogy, Encyclopedia of Ocean Sciences vol. 1. Elsevier, pp. 462–471.
Chumakov, N.M., 1995. The problem of the warm biosphere. Stratigr. Geol. Correl. 3, 205–215.
Collins, J.A., Schefuß, E., Heslop, D., Mulitza, S., Prange, M., Zabel, M., Tjallingii, R., Dokken, T.M., Huang, E., Mackensen, A., Schulz, M., Tian, J., Zarriess, M., Wefer, G., 2011. Interhemispheric symmetry of the tropical African rainbelt over the past 23,000 years. Nat. Geosci. 4, 42–45.
Conrad, C.P., 2013. The solid earth's influence on sea level. GSA Bull. 125, 1027–1052.
Elrick, M., Molina-Garza, R., Duncan, R., Snow, L., 2009. C-isotope stratigraphy and paleoenvironmental changes across OAE2 (mid-Cretaceous) from shallow-water platform carbonates of southern Mexico. Earth Planet. Sci. Lett. 277, 295–306.
Föllmi, K.B., 2012. Early Cretaceous life, climate and anoxia. Cretac. Res. 35, 230–257.
Francis, J.E., Ashworth, A., Cantrill, D.J., Crame, J.A., Howe, J., Stephens, R., Tosolini, A.-M., Thorn, V., 2008. 100 million years of Antarctic climate evolution: evidence from fossil plants. In: Cooper, A.K., Barrett, P.J., Stagg, H., Storey, B., Stump, E., Wise, W., the 10th ISAES editorial team (Eds.), Antarctica: A Keystone in a Changing World. The National Academy Press, Washington, D.C., pp. 19–28.
Galeotti, S., Rusciadelli, G., Sprovieri, M., Lanci, L., Gaudio, A., Pekar, S., 2009. Sea-level control on facies architecture in the Cenomanian–Coniacian Apulian margin (Western Tethys): a record of glacio-eustatic fluctuations during the Cretaceous greenhouse? Palaeogeogr. Palaeoclimatol. Palaeoecol. 276, 196–205.
Gertsch, B., Keller, G., Adatte, T., Berner, Z., Kassab, A., Tantawy, A., El-Sabbagh, A., Stueben, D., 2010. Cenomanian–Turonian transition in a shallow water sequence of the Sinai, Egypt. Int. J. Earth Sci. 99, 165–182.
Hallam, A., Grose, J.A., Ruffell, A.H., 1991. Palaeoclimatic significance of changes in clay mineralogy across the Jurassic–Cretaceous boundary in England and France. Palaeogeogr. Palaeoclimatol. Palaeoecol. 81, 173–187.
Haq, B.U., 2014. Cretaceous eustasy revisited. Glob. Planet. Chang. 113, 44–58.
Hasegawa, H., Tada, R., Jiang, X., Suganuma, Y., Imsamut, S., Charusiri, P., Ichinnorov, N., Khand, Y., 2012. Drastic shrinking of the Hadley circulation during the mid-Cretaceous Supergreenhouse. Clim. Past 8, 1323–1337.
Hay, W.W., Floegel, S., 2012. New thoughts about the Cretaceous climate and oceans. Earth Sci. Rev. 115, 262–272.
Hay, W.W., Leslie, M.A., 1990. Could possible changes in global groundwater reservoir cause eustatic sea level fluctuations? In: Geophysics Study Committee, C.o.P.S., Mathematics and Resources, National Research Council (Eds.), Sea Level Change: Studies in Geophysics. The National Academy of Sciences, National Academy Press, Washington D.C., pp. 161–170
Huber, B.T., Norris, R.D., MacLeod, K.G., 2002. Deep-sea paleotemperature record of extreme warmth during the Cretaceous. Geology 30, 123–126.
Jacobs, D.K., Sahagian, D.L., 1993. Climate-induced fluctuations in sea level during non-glacial times. Nature 361, 710–712.
Jacobs, D.K., Sahagian, D.L., 1995. Milankovitch fluctuations in sea level and recent trends in sea-level change: ice may not always be the answer. In: Haq, B.U. (Ed.), Sequence Stratigraphy and Depositional Response to Eustatic, Tectonic and Climatic Forcing, pp. 329–366.
Kidder, D.L., Worsley, T.R., 2010. Phanerozoic large igneous provinces (LIPs), HEATT (haline euxinic acidic thermal transgression) episodes, and mass extinctions. Palaeogeogr. Palaeoclimatol. Palaeoecol. 295, 162–191.
Laurin, J., Sageman, B.B., 2007. Cenomanian–Turonian coastal record in SW Utah, USA: orbital-scale transgressive-regressive events during Oceanic Anoxic Event II. J. Sediment. Res. 77, 731–756.
Laurin, J., Meyers, S.R., Uličný, D., Jarvis, I., Sageman, B.B., 2015. Axial obliquity control on the greenhouse carbon budget through middle to high latitude reservoirs. Paleoceanography http://dx.doi.org/10.1002/2014PA002736.
MacLeod, K.G., Huber, B.T., Berrocoso, Á.J., Wendler, I., 2013. A stable and hot Turonian without glacial δ18O excursions is indicated by exquisitely preserved Tanzanian foraminifera. Geology 41, 1083–1086.
Magaritz, M., Peryt, T.M., 1994. Mixed evaporite and meteoric water dolomitization: isotope study of the Zechstein Limestone (Upper Permian), southwestern Poland. Sediment. Geol. 92, 257–272.
Miller, K.G., Kominz, M.A., Browning, J.V., Wright, J.D., Mountain, G.S., Katz, M.E., Sugarman, P.J., Cramer, B.S., Christie-Blick, N., Pekar, S.F., 2005a. The Phanerozoic record of global sea-level change. Science 310, 1293–1298.
Miller, K.G., Wright, J.D., Browning, J.V., Paytan, A., 2005b. Visions of ice sheets in a greenhouse world. In: de la Rocha, C.L. (Ed.), Ocean Chemistry over the Phanerozoic and Its Links to Geological Processes. Marine Geology, pp. 215–231.
Moore, D.M., Reynolds Jr., R.C., 1997. X-ray Diffraction and the Identification and Analysis of Clay Minerals. Oxford University Press, Oxford.
Moriya, K., Wilson, P.A., Friedrich, O., Erbacher, J., Kawahata, H., 2007. Testing for ice sheets during the mid-Cretaceous greenhouse using glassy foraminiferal calcite from the mid-Cenomanian tropics on Demerara Rise. Geology 35, 615–618.
Morsi, A.-M.M., Wendler, J.E., 2010. Biostratigraphy, palaeoecology and palaeogeography of the Middle Cenomanian–Early Turonian Levant Platform in Central Jordan based on ostracods. Geol. Soc. Lond. Spec. Publ. 341, 187–210.
Mort, H.P., Adatte, T., Föllmi, K.B., Keller, G., Steinmann, P., Matera, V., Berner, Z., Stüben, D., 2007. Phosphorous and the roles of productivity and nutrient recycling during oceanic anoxic event 2. Geology 35, 483–486.
Pachur, H.-J., Kroplein, S., 1987. Wadi Howar: paleoclimatic evidence from an extinct river system in the South Eastern Sahara. Science 237, 298–300.
Peryt, T.M., Scholle, P.A., 1996. Regional setting and role of meteoric water in dolomite formation and diagenesis in an evaporite basin: studies in the Zechstein (Permian) deposits of Poland. Sedimentology 43, 1005–1023.
Petschick, R., Kuhn, G., Gingele, F.X., 1996. Clay mineral distribution in surface sediments of the South Atlantic: sources, transport, and relation to oceanography. Mar. Geol. 130, 203–229.
Pierre, C., Ortlieb, L., Person, A., 1984. Supratidal evaporitic dolomite at Ojo de Liebre lagoon: mineralogical and isotopic arguments for primary crystallization. J. Sediment. Petrol. 54, 1049–1061.
Richardt, N., Wilmsen, M., Niebuhr, B., 2013. Late Cenomanian–Early Turonian facies development and sea-level changes in the Bodenwöhrer Senke (Danubian Cretaceous Group, Bavaria, Germany). Facies 59, 803–827.
Schmidt, M.W., Spero, H.J., 2011. Meridional shifts in the marine ITCZ and the tropical hydrologic cycle over the last three glacial cycles. Paleoceanography 26 (PA1206).
Schulze, F., Marzouk, A.M., Bassiouni, M.A.A., Kuss, J., 2004. The late Albanian–Turonian carbonate platform succession of west-central Jordan: stratigraphy and crises. Cretac. Res. 25, 709–737.
Singer, A., 1984. The paleoclimatic interpretation of clay minerals in sediments; a review. Earth Sci. Rev. 21, 251–293.
Stoll, H.M., Schrag, D.P., 2000. High-resolution stable isotope records from the upper cretaceous rocks of Italy and Spain: glacial episodes in a greenhouse planet? Geol. Soc. Am. Bull. 112, 308–319.
Thiry, M., 2000. Palaeoclimatic interpretation of clay minerals in marine deposits: an outlook from the continental origin. Earth-Sci. Rev. 49, 201–221.
Trenberth, K.E., Smith, L., Qian, T., Dai, A., Fasullo, J., 2007. Estimates of the global water budget and its annual cycle using observational and model data. Special Section—J. Hydrometeorol. Spec. Sec. 8, 758–769.
Tucker, M., 1988. Techniques in Sedimentology. Blackwell Scientific Publications, Oxford.
van Helmond, N.A.G.M., Sluijs, A., Reichart, G.-J., Sinninghe Damsté, J.S., Slomp, C.P., Brinkhuis, H., 2014. A perturbed hydrological cycle during Oceanic Anoxic Event 2. Geology 42, 123–126.
Vogt, C., Lauterjung, J., Fischer, R.X., 2002. Investigation of the clay fraction (<2 μm) of the clay mineral society reference clays. Clay Clay Miner. 50, 388–400.

Voigt, S., Gale, A.S., Voigt, T., 2006. Sea-level change, carbon cycling and palaeoclimate during the Late Cenomanian of northwest Europe; an integrated palaeoenvironmental analysis. Cretac. Res. 27, 836–858.
Wagreich, M., Lein, R., Sames, B., 2014. Eustasy, its controlling factors, and the limno-eustatic hypothesis—concepts inspired by Eduard Suess. Aust. J. Earth Sci. 107, 115–131.
Wendler, J.E., Wendler, I., 2016. What drove sea-level fluctuations during the mid-Cretaceous greenhouse climate? Palaeogeogr. Palaeoclimatol. Palaeoecol. 441, 412–419.
Wendler, J.E., Lehmann, J., Kuss, J., 2010. Orbital time scale, intra-platform basin correlation, carbon isotope stratigraphy, and sea level history of the Cenomanian/Turonian Eastern Levant platform, Jordan. Geol. Soc. Lond. Spec. Publ. 341, 171–186.
Wendler, J.E., Meyers, S.R., Wendler, I., Vogt, C., Kuss, J., 2011. Drivers of cyclic sea level changes during the Cretaceous greenhouse: a new perspective from the Levant Platform. Geol. Soc. Lond. Spec. Publ. 43, 376.
Wendler, J.E., Meyers, S.R., Wendler, I., Kuss, J., 2014. A million-year-scale astronomical control on Late Cretaceous sea-level. Newsl. Stratigr. 47, 1–19.
Wendler, I., Wendler, J.E., Clarke, L.J., 2016. Sea-level reconstruction for Turonian sediments from Tanzania based on integration of sedimentology, microfacies, geochemistry and micropaleontology. Palaeogeogr. Palaeoclimatol. Palaeoecol. 441, 528–564.